Contrib. Plasma Phys. **45**, No. 5-6, 338 – 347 (2005) / **DOI** 10.1002/ctpp.200510039

Cross-Correlation Spectroscopy Applied to the Investigation of Barrier Discharges in N_2/O_2 Mixtures at Atmospheric Pressure

H.-E. Wagner [*1], **R. Brandenburg** [**1], **K. V. Kozlov** [2], **A. M. Morozov** [2], and **P. Michel** [1]

[1] Institute of Physics, Ernst-Moritz-Arndt University of Greifswald, Domstr. 10a, 17489 Greifswald, Germany
[2] Moscow State University, Department of Chemistry, Leninskie Gory 1, Str.3, 119899 Moscow, Russia

Received 09 May 2005, accepted 13 June 2005
Published online 29 July 2005

Key words Barrier discharge, filamentary, diffuse, N_2/O_2 mixtures, spectroscopy, microdischarge development, elementary processes.
PACS 52.70.Kz, 50.70.Ds, 52.80.Tn

The techniques of spatially resolved cross-correlation spectroscopy (CCS) and current pulse oscillography were used to carry out systematic investigations of the barrier discharge (BD) in the binary gas mixtures N_2/O_2 at atmospheric pressure. In the case of the BD filamentary mode, which is characterized by the formation of microdischarges (MDs) of short duration, the spatio-temporal distributions of the BD radiation intensities were recorded for the spectral bands of the 0-0 transitions of the 2^{nd} positive (λ= 337 nm) and 1^{st} negative system of molecular nitrogen (λ= 391 nm). The velocities of the cathode-directed ionising waves as well as the effective lifetimes of the excited states $N_2(C^3\Pi_u)_{v'=0}$ and $N_2^+(B^2\Sigma_u^+)_{v'=0}$ were evaluated from the CCS data. The two-dimensional optical scanning of the MD channel (in axial and radial directions of the MD) was carried out for the BD operated in the gas mixture consisting of 6 vol.% of O_2 and 94 vol.% of N_2. In the middle of gap, the MD channel diameter was found to be about 0.3 mm and to expand towards both electrodes. On the dielectrics, outward propagating discharges were observed. In pure nitrogen the diffuse mode of barrier discharge was investigated. Surprisingly, under the conditions studied, the transition to the filamentary mode already starts for O_2 admixtures to nitrogen of $\geq$ 400 ppm.

1 Introduction

Experimental and theoretical studies on the breakdown in barrier discharges (BDs) have a long history [1] - [5]. However, despite of the considerable progress in the understanding, the knowledge of this subject nowadays appears to be insufficient to provide an adequate quantitative description. Main reasons for this situation are the difficulties to investigate experimentally the dynamics of these usually filamentary plasmas, requiring a sub-ns temporally and sub-mm spatially resolution. While the last two periods within the project A 10 "Kinetics of reactive plasmas under non-stationary and non-homogeneous conditions up to one bar" of the collaborative research centre 198, "Kinetics of partially ionized plasmas", BDs have been investigated by our team. As a first step, the technique of spatially resolved cross-correlation spectroscopy (CCS) was established in Greifwald. Namely, results on the spatio-temporally resolved spectroscopic diagnostics along the axis of single microdischarges (MDs) in air at atmospheric pressure were sufficient for the quantitative estimation of the local electric field strength and relative electron density in air at atmospheric pressure [6] [7]. Both key plasma parameters are summarized in the figure 1 and characterize the starting point of the second period of founding.

Our recent activities (2002 - 2004) were focused on a systematic study of the BD behaviour in binary N_2/O_2 gas mixtures which will be summarized in this paper. We intended to clarify the role of the working gas electronegativity in the discharge mechanism. Surprisingly, we did not find any qualitative change in the spatio-temporal structure of the MDs in a wide range of oxygen concentrations (namely, from 97 vol.% down to 0.5 vol.%). Since the CCS is a single-photon accumulation technique, a high reproducibility and long-time

* Corresponding author: e-mail: wagner@physik.uni-greifswald.de, Phone: +00 49 3834 864745, Fax: +00 49 3834 864701
** currently at Institute of Low-Temperature Plasma-Physics (INP), Greifswald

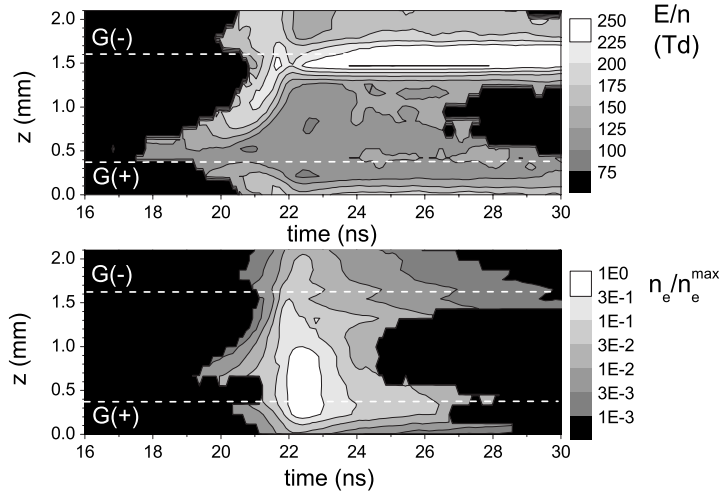

Fig. 1 Distributions of the electric field and electron density in synthetic air. The positions of the tips of the glass surfaces are indicated by $G(-)$ and $G(+)$; operation conditions: p= 1 bar, f= 6.5 kHz, U_{pp}= 12 kV [6]. A value $n_e^{max} \approx 10^{12}\ cm^{-3}$ has been derived from current pulse measurements [7].

stability of the repetitive MDs is required to perform axially and radially resolved CCS measurements. However, under selected operation conditions such experiments were possible as presented in this contribution, too.

In the N_2/O_2 mixtures with O_2 content below 500 ppm, we found a BD operating in a diffuse mode (also referred to as atmospheric pressure glow discharge, glow silent discharge [8] or homogeneous barrier discharge [9]). Therefore, we extended our attention on the diffuse mode of the BD, in order to contribute to a better understanding of the mechanism of this discharge type by means of the spatio-temporally resolved spectroscopic diagnostics provided by the CCS apparatus.

Only a few important aspects of the experimental technique are outlined in the section 2 of this paper, since the corresponding full and detailed description of the apparatus and procedure of the CCS measurements is presented in the previous papers [6, 10, 11]. In the section 3, the experimental results are reported for the filamentary mode of BDs (sub-section 3.1), reporting the influence of the binary gas mixture ratio on the velocity of the ionisation wave and the current pulse shape, and the axial and radial development of MDs. Selected results on the transition between the filamentary and diffuse mode of BDs are summarized in sub-section 3.2.

2 Experimental set-up

The experimental equipment was described elsewhere, e.g. in [6, 11]. In order to localize repetitive single MDs, the BDs were generated between two semi-spherical electrodes, both covered by glass. The electrodes were mounted with a gap distance g within the range 0.9 and 2.2 mm (see figure 2, (a)). This electrode arrangement provided the possibility to observe not only the volume part of the MD, but also the surface discharge processes. In order to compare the experimental results on diffuse BDs with numerical modelling results, a planar discharge cell configuration was used for this part of the investigations (figure 2, (b)). In each case the discharge cells were placed in a vacuum chamber which was evacuated down to about 0.1 mbar before each experiment. The BD was driven by sinusoidal voltage (frequency f= 6.9 kHz, peak-to-peak amplitude U_0= 12 ... 19 kV). The working gas composition was realised by means of mass-flow controllers (MKS, 1259 CC), provided that the total gas flow rate was maintained at about 40 l h^{-1}. Additional to optical emission spectroscopy and CCS the single MD current pulse measurements were performed by the fast-current probe (Tektronix, CT-1) and an oscilloscope (Tektronix, TDS 380).

In the following, a brief review on the technique of spatially resolved CCS is given. The set-up is shown schematically in the figure 3. By means of a quartz lens, the discharge zone was imaged onto an optical slit. By appropriate adjustment and movement of this slit, the discharge area could be scanned in vertical (r) and horizontal (z) directions (resolution not worse than 0.1 mm). The localized radiation (so-called "main signal") was resolved spectrally by a monochromator (Triax 320, ISA Jobin Yvon). The monochromatic light was detected by the high-gain photo-multiplier (PMT), which operated in a single photon counting mode (H5773-04, Hamamatsu). The second detector for the synchronizing ("sync") signal was adjusted so as to reach the maximal possible temporal resolution of the steep front of a light pulse, since the derivative of this signal was actually used

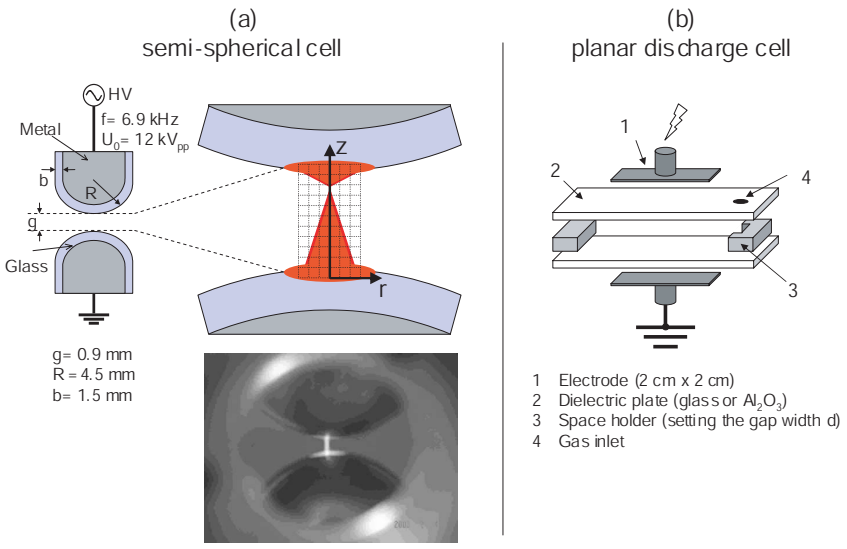

Fig. 2 (a) Principal scheme of the discharge cell with indicated area of axial and radial optical scanning and a photo of the discharge cell with the localised repetitive MDs. (b) Schema of the planar discharge cell. (Online colour: www.cpp-journal.org).

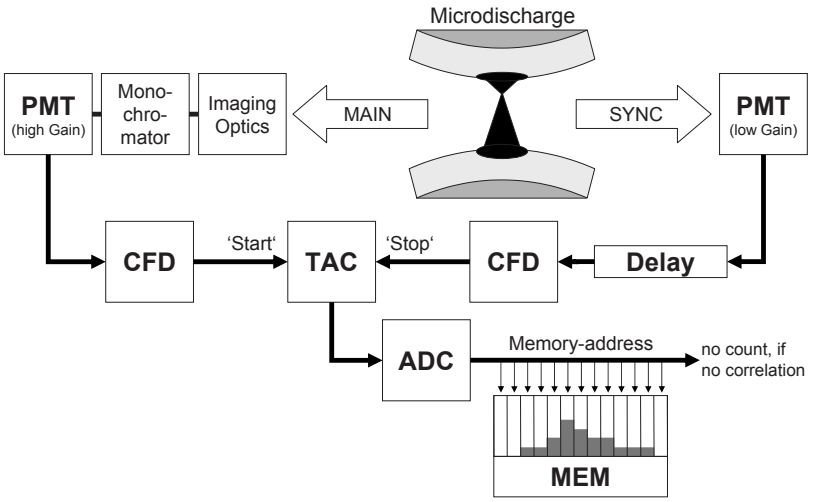

Fig. 3 An outline of the CCS-apparatus and measurement procedure (the "reversed start-stop" mode is shown). Abbreviations: PMT, photomultiplier; CFD, constant fraction discriminator; TAC, time-to-amplitude converter; ADC, analogue-to-digital converter; MEM, memory.

to define a zero-point of the relative time scale (so-called optical triggering procedure). The measurements of the correlation functions and accumulation of the results were carried out by the time correlated single photon counting (TC-SPC) board (SPC-530, Becker and Hickl GmbH). The basic components of the TC-SPC instrument are two constant fraction discriminators (CFD), a time-to-amplitude converter (TAC), an analog-to-digital converter (ADC) and a memory (MEM). The discriminators are used to select electric pulses which belong to a pre-defined range of the amplitudes. A selected pulse of the main signal initiates a linear rise of the voltage of the TAC, and a first following selected pulse of the sync signal stops this rise. The value of the measured quantity (voltage amplitude) is converted to the number of the corresponding time channel of the device (actually, to a memory

address) by the ADC and the number of counts of the adressed MEM-channel is increased by one. The entire scale of a memory segment consists of 1024 channels. If no synchronizing signal comes and the voltage of the TAC reaches its upper limit, then no count is registered in the MEM-segments. A correspondence between the time value and the number of the time channel is determined by the duration of the voltage rise, which is variable from 50 ns to several μs. A shift of zero-point to the left over time axis is possible due to the insertion of the coaxial delay-cable between the detector for sync signal and the TC-SPC module (so-called "reversed start-stop" mode of CCS). Typically, up to 10^7 counts were accumulated in the memory segment with a maximal count rate for a measurement of 5 minutes of duration. The temporally resolved intensity distribution was recorded with a time resolution of about 0.1 ns. Additionally the MEM-segments are controlled by a pattern-generator (PPG-530, Becker and Hickl GmbH) in order to resolve the measurements along the phase of the applied voltage (not shown in the figure 3). This feature of the experimental apparatus makes it possible to investigate diffuse BDs, too. The neccessary modifcations of the set-up are described in [12, 13].

3 Results and discussion

3.1 Filamentary barrier discharges

3.1.1 Systematic variation of N_2/O_2 mixtures

In order to investigate the influenece of electronegativity of working gas on the mechanism of BD development, systematic CCS-measurements of the MD luminosities for several binary mixtures (N_2/O_2) were carried out within 0.5 - 97 vol% admixture of oxygen to nitrogen [12]. The spatio-temporal distributions of the MD radiation intensities were recorded for the spectral bands of the 0-0 transitions of the 2^{nd} positive (SPS, (1)) and 1^{st} negative system of molecular nitrogen (FNS, (2)).

$$N_2(C^3\Pi_u)_{v'=0} \rightarrow N_2(B^3\Pi_g)_{v''=0} + \frac{hc}{\lambda_C} \qquad \lambda_C = 337.1\,nm \tag{1}$$

$$N_2^+(B^2\Sigma_u^+)_{v'=0} \rightarrow N_2^+(X^2\Sigma_u^+)_{v''=0} + \frac{hc}{\lambda_B} \qquad \lambda_B = 391.5\,nm \tag{2}$$

Surprisingly, for all these mixtures the same characteristic features of the MD luminosity distributions as for air [6] were observed. The trajectories of the cathode-directed ionisation waves can be easily revealed from the plots of spatio-temporal distributions of the MD radiation intensity for FNS. An example of such a presentation is shown in figure 4 together with the indicated trajectory of the cathode-directed ionisation wave. In this easy way (determination of the gradient of the maximum luminosity) the local velocities of the cathode-directed ionisation waves were determined. Figure 5 demonstrates that on most of the pathway from the anode to the cathode, the ionisation waves propagate with exponentially growing velocities (considered as functions of the distance from the anode surface). The maximum velocity of the cathode directed ionisation wave is about v= 2 10^6 m s^{-1} [12]. Under the conditions being considered and within the limits of our experimental accuracy, no noticeable influence of oxygen content upon the propagation of the cathode-directed ionising waves can be observed. These results allow us to conclude that within this concentration range, the mechanism of the MD development does not change significantly.

Contrary to this, the last phase of the MD development (the "phase of decay", see [6]) depends on the composition of the binary N_2/O_2 mixtures. This dependence can be clearly seen from the results of the MD current pulse measurements (figure 6). As higher the oxygen concentration as shorter the MD current pulses. Their dependence upon the oxygen content can be explained as follows. During the decay phase of the MD development, most of the electrons are in the region with a low and slowly decreasing electric field [6]. Under such conditions, the electrons disappear from the MD channel not only because of their drift and transition onto the anode surface, but due to electron attachment as well. Obviously, the greater the oxygen concentration, the higher is the electron attachment rate. The current pulse amplitude has been found to be a growing function of oxygen content within the range 0.2-10 vol.% and a decreasing one for oxygen concentrations greater than 10 vol.%. It is difficult to propose a simple explanation for such behaviour of the current pulse amplitudes, since the latter quantities are determined by the parameters of ionisation waves.

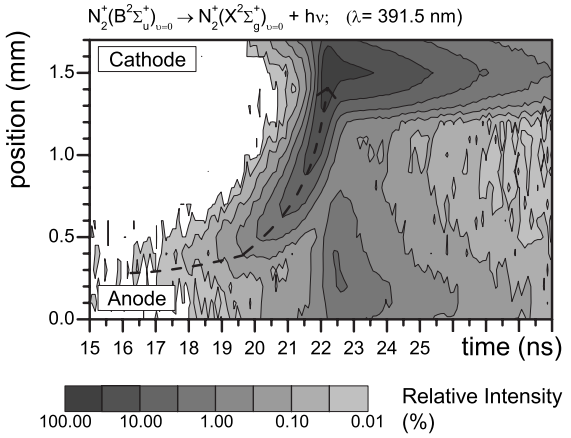

Fig. 4 Example of the measured spatio-temporal distribution of the MD luminosity for FNS (λ= 391.5 nm) with the indicated trajectory of the cathode-directed ionising wave.

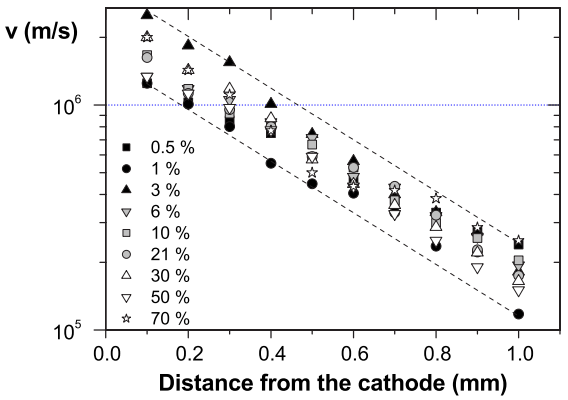

Fig. 5 Velocities of the cathode-directed ionising waves in the N_2/O_2 mixtures of different compositions (oxygen percentages are indicated in the legend).

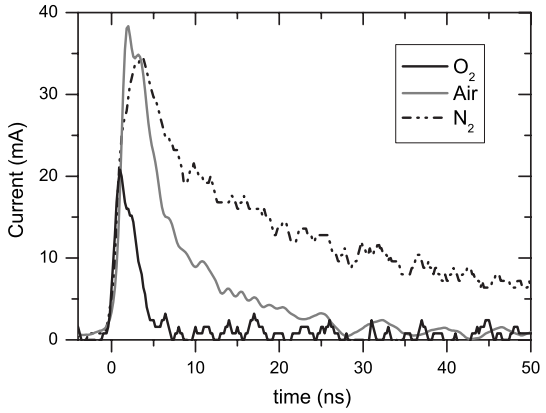

Fig. 6 MD current pulses in N_2, air and O_2 (experimental parameters as in figure 5).

3.1.2 Determination of the effective lifetimes of the states $N_2^+(B^2\Sigma_u^+)_{\upsilon'=0}$ and $N_2(C^3\Pi_u)_{\upsilon'=0}$

In the case of the light pulses, the values of the decay rates can be determined from the experimentally obtained spatio-temporal distributions of the MD luminosity. These local decay rates should be treated as functions of the two variables: position (r) and time (t). In order to perform such analysis of our CCS measurement data, first of all we have to consider the basic elementary processes determining the MD radiation kinetics. According to the literature the following groups of elementary processes should be taken into account to describe the radiation kinetics for SPS and FNS (0-0 transitions) at atmospheric pressure. A detailed discussion of the elementary processes and the kinetic scheme has been undertaken in [6, 12]

- Excitation of the molecules of nitrogen (in the ground state $N_2(X^1\Sigma_g^+)_{\upsilon=0}$) to the states $N_2(C^3\Pi_u)_{\upsilon'=0}$ and $N_2^+(B^2\Sigma_u^+)_{\upsilon'=0}$ by direct electron impact
- Spontaneous radiation of thus formed excited species
- Collisional quenching of the excited species by the molecules of nitrogen and oxygen

The results on the dependencies of the effective lifetimes of the states $N_2^+(B^2\Sigma_u^+)_{\upsilon'=0}$ and $N_2(C^3\Pi_u)_{\upsilon'=0}$ on the oxygen content are summarized in figure 7. This figure shows that these estimates appear to be very close to the curves obtained by direct calculation using the values of the collisional quenching rate constants

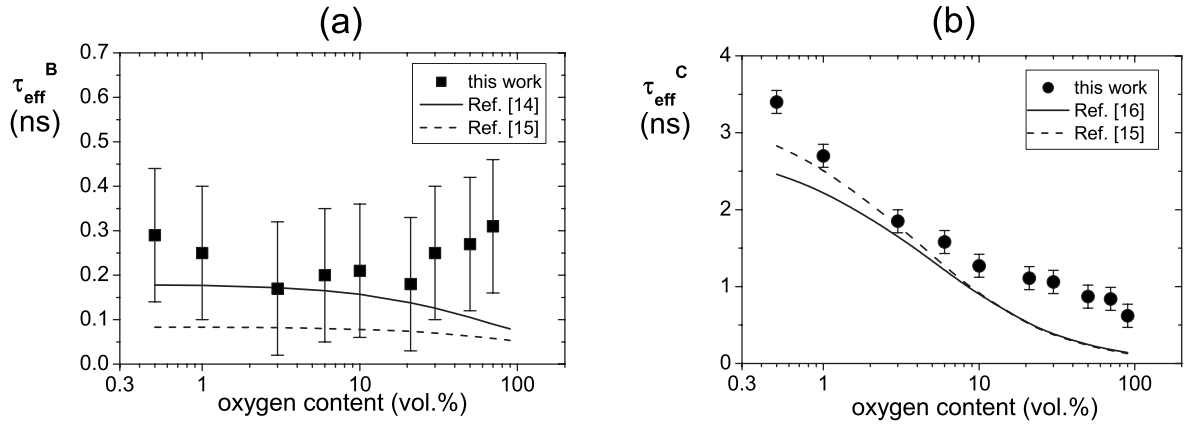

Fig. 7 Dependencies of the effective lifetimes of the states a) $N_2^+(B^2\Sigma_u^+)_{v'=0}$ and b) $N_2(C^3\Pi_u)_{v'=0}$ denoted as τ_{eff}^B and τ_{eff}^C, respectively, on the oxygen content.

selected from the literature (an overview of these kinetic data is presented in [6, 12]). In the case of the FNS, no noticeable influence of the oxygen concentration on the effective lifetime τ_{eff}^B is observed (see figure 7(a)). For the SPS, an increase in oxygen content results in a considerable decrease of the τ_{eff}^C values (figure 7(b)). These dependencies are actually determined by the values of the rate constants of collisional quenching of the radiating species $N_2(C^3\Pi_u)_{v'=0}$ and $N_2^+(B^2\Sigma_u^+)_{v'=0}$ by the molecules N_2 and O_2. At this example it has been demonstrated that the techniques of CCS is an useful tool for the estimation of quenching rate constants, too.

3.1.3 Axial and radial development of single microdischarges

For the first time, the two-dimensional optical scanning of the MD channel (in axial and radial directions of the MD) was carried out for the BD operated in the gas mixture consisting of 6 vol.% of O_2 and 94 vol.% of N_2 [7,11]. This gas composition had been found to provide extremely high stability of the discharge that was necessary for the time-consuming scanning procedure. Since the development of the MD proceeds in a similar way in all binary gas mixtures of N_2 and O_2 considered in the prevoius sections, the results for the above-mentioned mixture can be seen as being representative for the entire concentration range. For the (0-0) transition of the SPS at λ= 337.1 nm, the evolution of the axially and radially resolved distributions of the MD luminosity (radiation intensity) is shown in figure 8. The presented results are up to now integrated measurements over the MD channel depth. Therefore, the local intensities can be somewhat modified. Nevertheless, these results visualize the phases of the discharge development in impressive manner, imaging the volume situation as well as the discharge propagation on the dielectric surfaces. In figure 8 the following subsequent phases of the MD development can be distinguished.

(I) The MD starts with a Townsend pre-breakdown phase (figure 8, (a)), lasting for more than 150 ns [6]. At this time no significant space charges has been formed yet, and the maximum of light intensity is observed at the anode surface. It should be noted that the radial distribution of the intensity is not uniform. Only a small area of the dielectric is covered. The position of the MD seems to be determined by the residual charges on the dielectrics deposited in their predecessor.

(II) The light intensity at the anode increases in time (figure 8, (b)). When a sufficient positive space charge has grown up in front of the anode the cathode directed ionising wave starts to propagate. The ionisation wave is caused by the local distortion of the electric field and moves with an acceleration towards the cathode (figure 8, (c)-(e)). At this time, the value of the MD channel diameter (i.e. the value of the FWHM of radial intensity distribution) is about 0.3 mm. In the backward area of the ionising wave, electrons drift towards the anode, generating a glow near the anode. Thus two light spots are clearly seen in figure 8, (e). These spots correspond to two active zones of the MD with different properties: the region near the cathode is characterized by higher electric field [6]. Additionally, our previous results [6] have indicated that the density of electrons near the cathode in opposite is smaller than at the anode (see figure 1).

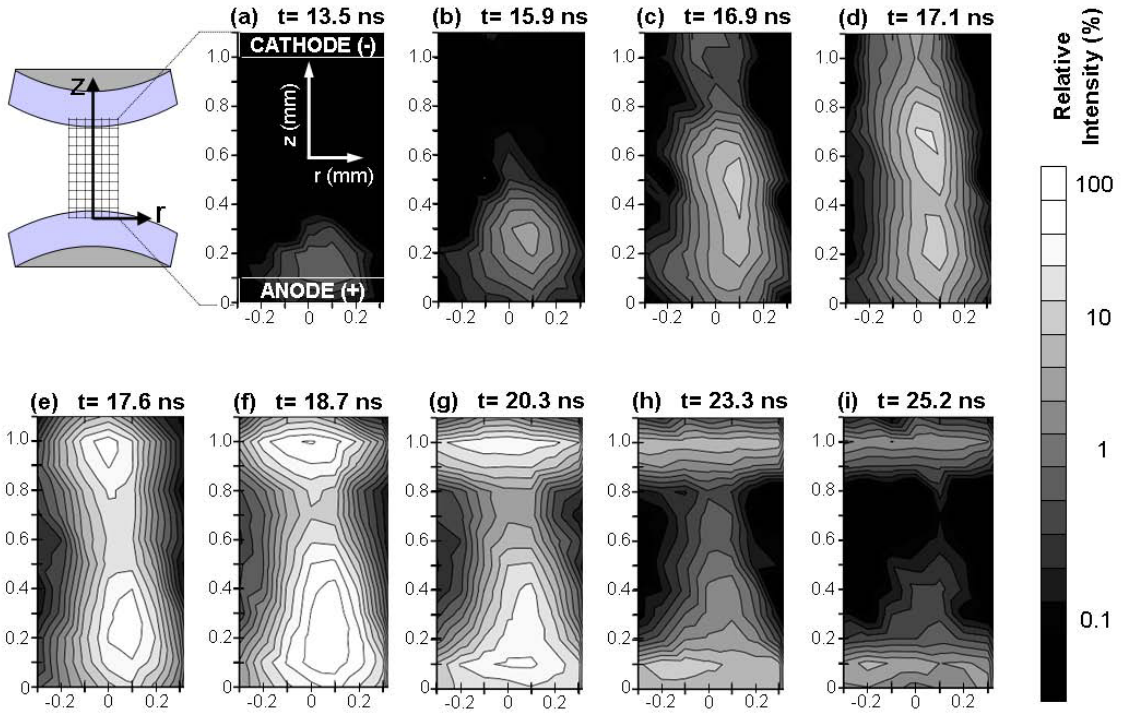

Fig. 8 Evolution of the light intensity distributions for MDs in the mixture of N_2 (94 vol.%) and O_2 (6 vol.%) (SPS, (0-0) transition at 337 nm).

(III) The ionisation wave crosses the discharge gap within about 3 ns. At the same time when they reaches the cathode the anode glow has been developed. At this stage of the MD development charge carriers are accumulated on the electrodes much faster than during the previous phases. Therefore, the radial component of the electric field increases and causes considerable broadening of the MD channel at the electrodes. The values of the corresponding diameters on the surface become comparable to the discharge gap width (figure 8, (f)).

(IV) The MD decays within a period of about 10 ns (figure 8, (g)-(i)) due to the reduction of axial electric field caused by accumulation of charge carriers on the dielectrics. This general decay is accompanied by the propagation of the surface discharges. The ratio betwen the propagation velocities of the discharge on the surface to that in the volume is about 0.1.

3.2 Transition between the filamentary and diffuse mode of barrier discharges

When the BD was operated in pure nitrogen, it looked like two round luminous diffuse spots of a few millimetre diameter, located on the spherical electrode surfaces. General, a transition from the diffuse to the filamentary mode can be caused by an increase in the driving voltage amplitude, by a variation of the voltage frequency (diffuse mode of the BD is stable within certain frequency limits, only), or by impurities in the working gas (see [12, 13]) and refernces therein). The diffuse mode of the BD was found to be stable in pure nitrogen (the content of impurities $<$ 10 ppm) as well as in the binary mixtures N_2/O_2 at oxygen concentrations below 400 ppm. The transition between the two modes has been extensively investigated in a discharge cell with planar electrodes covered by glass barriers (electrode area: 2x2 cm^2, gap=1.1 mm) [13]. The time dependencies of the active current for different external admixtures of O_2 are shown in figure 9. Up to 90 ppm of O_2 in N_2 an increase of amplitude and duration of the active current peak is investigated. For higher oxygen content the current decreases. At about 480 ppm regular oscillations in the current pulse are observed. These oscillations

mark the transition to the filamentary mode. Increasing the O_2 content the instabilities get more pronounced. For 800 ppm of O_2 in N_2 MDs are observed as shown in the seperated part of figure 9.

It is accepted that a Townsend-breakdown is responsible for the ignition of a diffuse BD in nitrogen [8]. The decisive criterion for this is the presence of charge carriers at low electric field, i.e. a "memory effect" producing primary electrons below the breakdown voltage. In the literature different processes for the production of seed primary electrons are controversially discussed. In particular, the importance of volume and surface processes on the pre-ionisation and the role of surface charges are the subjects of discussion. Penning ionisation, due to collision of nitrogen metastable states $N_2(A^3\Sigma_u)$ and $N_2(a'^1\Sigma_u^-)$ was the first process suggested in literature [17]. The much more effecitive quenching of the metastable states by oxygen molecules according to the reaction $O_2 + N_2(A^3\Sigma_u^+) \rightarrow N_2(X^1\Sigma_g^+) + O + O$ than by nitrogen (the rate constants differ about seven order of magnitudes) should explain the transition from the diffuse to the filamentary BD by the admixture of O_2 [11]. But nevertheless, due to quenching of $N_2(a'\Sigma_u^-)$ molecules by nitrogen molecules the indirect ionisation rate via Penning ionisation appeared to be too low to sustain a diffuse BD. Therefore, to explain the experimental results by numerical models, secondary electron emission by $N_2(A^3\Sigma_u)$-metastable states had to be included [13, 18]. Selected examples on the spatio-temporally distribution in the diffuse mode of BD are summarized in figure 10. It presents the distribution of the relative radiation intensity for different spectral lines (parts (a) and (b)) as well as calculated density distributions (parts (c) and (d)). The spectral transitions of the SPS of N_2 (1) and the NO_γ system (3) have been chosen.

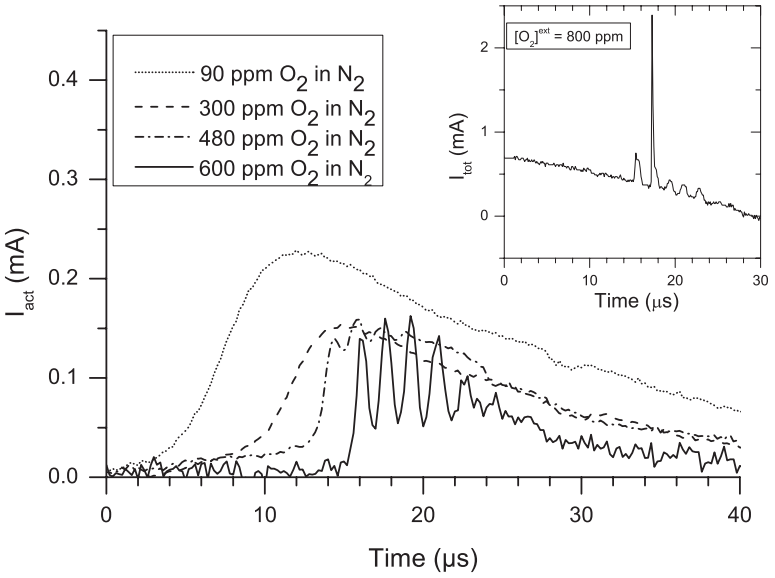

Fig. 9 Active discharge5 current I_{act} for different gas compositions, demonstrating the transition of the diffuse BD to the filamentary mode. See [12, 13] for details.

$$NO(A^2\Pi^+)_{v'=0} \rightarrow NO(X^2\Pi)_{v''=3} + \frac{hc}{\lambda_g} \qquad \lambda_g = 259.6\,nm \tag{3}$$

In figure 10 the time scale slightly exceeds one period of the applied voltage T and the time resolution of the experimental results (parts (a) and (b)) is 1.1 μs. Of course, there are quite different time scales of the discharge period T, compared with the filamentary mode. In the first half of period the anode is located at the top and vice versa. The scale of relative intensity is grey-coded from white to grey in logarithmic steps in order to cover up to four orders of magnitudes of the signal. In the same way as the intensity distributions, the calculated density profiles of the radiating specie $N_2(C^3\Pi_u)$ and the metastable state $N_2(A^3\Sigma_u)$ are shown (parts (c) and (d)). Assuming a constant distribution of NO over the entire discharge volume after some time of operation the calculated $N_2(A^3\Sigma_u)$-profiles can be compared with the NO_γ-signal. A reasonable qualitative spatio-temporally agreement between measured and calculated profiles is achieved. The results in figure 10 clearly show the "Townsend-like" character of the diffuse BD in nitrogen: The electron density increases towards the anode exponentially, while the local electric field is not drastically distorted by space charges. As a consequence an exponential growth of the intensity of the SPS is investigated. The distribution of the radiation intensity for NO_γ is determined by the

profile of $N_2(A^3\Sigma_u)$ density. Its relatively long lifetime relative to the quenching by O_2 molecules causes the slower decay of the intensity peaks.

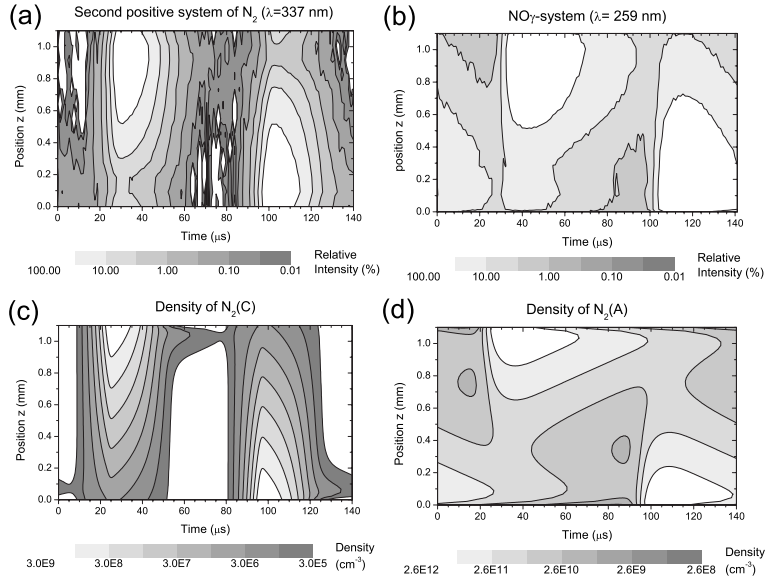

Fig. 10 Measured intensity distributions of the 0-0 transition of the SPS of N_2 (λ_C= 337.1 nm) (a) and the 0-3 transition of the NO_γ system (λ_g= 259.6 nm) (b), compared with calculated density profiles of the radiating species N_2(C) (c) and N_2(A) (d) in the gas mixture of 300 ppm O_2 in N_2. Taken from [13]

4 Conclusions

The cross correlation emission spectroscopy (CCS) is a powerful tool to analyze spectrally resolved the spatio-temporal structure of BDs in the filamentary mode (with a sub-ns and sub-mm resolution) as well as in the diffuse mode. The arrays of experimental results are sufficient for the quantitative estimation of the local electric field strength and the relative electron density under these conditions.

For the first time, the two-dimensional spectrally resolved scanning of the MD channel (in axial and radial directions of the MD) was carried out for the BD operated in the gas mixture consisting of 6 vol.% of O_2 and 94 vol.% of N_2. These results visualize in detail the phases of the discharge development in the volume and on the dielectric surfaces: Townsend pre-breakdown phase on the anode, ionisation wave crossing the gap from the anode to the cathode and decay phase on the dielectric surfaces. It was found that the ratio betwen the propagation velocities of the discharge on the surface to that in the volume is about 0.1 under the conditions being considered.

By the CCS the determination of the effective lifetimes of the states $N_2^+(B^2\Sigma_u^+)_{v'=0}$ and $N_2(C^3\Pi_u)_{v'=0}$ was possible. The results appear to be very close to the curves obtained by direct calculation using the values of the collisional quenching rate constants selected from the literature. At oxygen concentrations greater than 500 ppm, the BD exists in the filamentary mode, only. A variation of the oxygen content within this concentration range does not cause any qualitative changes of the MD development mechanism, and it does not exert any noticeable influence on the velocities of the cathode-directed ionising waves. The duration of the MD decay phase decreases monotonously with an increase of oxygen content. This phase was found to be determined by electron attachment and collisional quenching of excited states by molecular oxygen and nitrogen.

At oxygen concentrations less than 400 ppm, the BD operates in the diffuse mode, provided that the driving voltage amplitude is sufficiently low. The spatio-temporal distributions of the light intensity for the selected spectral bands correspond to the Townsend mechanism of the discharge development. The kinetic modelling of the diffuse mode underlines the dominant role of metastable nitrogen molecules. In particular, secondary electron emission by $N_2(A^3\Sigma_u)$-metastable states had to be included in order to explain the transition between filamentary and diffuse BD-modes in N_2/O_2 mixtures.

Acknowledgements This work was supported by the Deutsche Forschungsgemeinschaft (DFG), Sonderforschungsbereich 198: "Kinetics of partially ionised plasmas".

References

[1] Series in Plasma Physics: Non-Equilibrium air plasmas at atmospheric pressure, Eds. K.H. Becker, U. Kogelschatz, K.H. Schönbach, R.J. Barker, IOP Publishing LTD (2005).

[2] U. Kogelschatz Dielectric-barrier discharges: Their history, discharge physics, and industrial applications, *Plasma Chemistry and Processing* **23** 1, 1-45 (2003).

[3] V.G. Samoilovich, V.I. Gibalov, K.V. Kozlov 1997 *Physical chemistry of the barrier discharge (Düsseldorf: DVS)*

[4] H.-E. Wagner, R. Brandenburg, K.V. Kozlov, Progress in the Visualization of Filamentary Gas Discharges, Part 1: Milestones and Diagnostics of Dielectric-barrier Discharges by Cross-correlation Spectroscopy, *Journal of Advanced Oxidation Technologies*, Vol. **7** No. 1, 11-19 (2004).

[5] H.-E. Wagner , R. Brandenburg, K.V. Kozlov, A. Sonnenfeld, P. Michel, J.F. Behnke, The barrier discharge: basic properties and applications to surface treatment *Vacuum* **71** No 3, 417-436 (2003).

[6] K.V. Kozlov, H.-E. Wagner, R. Brandenburg, P. Michel, Spatio-temporally resolved spectroscopic diagnostics of the barrier discharge in air at atmospheric pressure *J. Phys.D: Appl. Phys.* **34**, 3164-3176 (2001).

[7] R. Brandenburg, Räumlich und zeitlich aufgelöste spektroskopische Untersuchungen an filamentierten und diffusen Barrierenentladungen, Dissertation, University of Greifswald (2004) (in German)

[8] N. Gherardi, G. Gouda, E. Gat, A. Ricard, F. Massines, Transition from glow silent discharge to micro-discharges in nitrogen gas, *Plasma Sources Sci. Technol.* **9**, 340-346 (2000).

[9] Yu.B. Golubovskii, V.A. Maiorov, J. Behnke, J.F. Behnke, Influence of interaction between charged particles and dielectric surface over an homogeneous barrier discharge in nitrogen *J. Phys.D: Appl. Phys.* **35**, 751-761 (2002).

[10] K.V. Kozlov, V.V. Dobryakov, A.P. Monyakin, V.G. Samoilovich, O.S. Shepeliuk, H.-E. Wagner, R. Brandenburg, P. Michel, Cross-correlation spectroscopy in investigations of filamentary gas discharges at atmospheric pressure *Selected Research Papers on Spectroscopy of Nonequilibrium Plasma at elevated Pressures (Proceedings of SPIE)* vol **4460**, Eds V.N. Ochkin (Washington), 165-176 (2002),

[11] R. Brandenburg, H.-E. Wagner, A.M. Morozov, K.V. Kozlov, Axial and radial development of the microdischarges of barrier discharge in N_2/O_2 mixtures at atmospheric pressure, *J. Phys.D: Appl. Phys.* **38**, 1649-1657 (2005), Special Issue: Microplasmas

[12] K.V. Kozlov, R. Brandenburg, H.-E. Wagner, A.M. Morozov, P. Michel, Investigation of the filamentary and diffuse mode of barrier discharges in N_2/O_2 mixtures at atmospheric pressure by cross-correlation spectroscopy, *J. Phys.D: Appl. Phys.* **38**, 518-529 (2005), Special issue on atmospheric pressure non-thermal plasmas for processing and other applications

[13] R. Brandenburg, V.A. Maiorov, Yu.B. Golubovskii, H.-E. Wagner, J. Behnke, J.F. Behnke, Diffuse barrier discharges in nitrogen with small admixtures of oxygen: discharge mechanism and transition to the filamentary regime, *J. Phys.D: Appl. Phys.* **38**, 2187-2197 (2005).

[14] S.V. Pancheshnyi, S.M. Starikovskaia, A.Yu. Starikovskii, Measurement of the rate constants of collisional quenching of $N_2(C^3\Pi_u)$ and $N_2^+(B^2\Sigma_u^+)$ by the molecules N_2, O_2 and CO in afterglow of the nanosecond discharge *Sov. Plasma Phys.* **23** 7, 664-669 (1997).

[15] J.M. Calo, R.C. Axtmann, Vibrational relaxation and electronic quenching of the $C^3\Pi_u(\upsilon'=1)$ state of nitrogen *J. Chem. Phys.* **54**, 1332-1341 (1971).

[16] F. Albugues, A. Birot, D. Blanc, H. Brunet, J. Galy, P. Millet, J.L. Teyssier, Destruction of the levels $C^3\Pi_u(\upsilon'=0, \upsilon'=1)$ of nitrogen by O_2, CO_2, CH_4, and H_2O, *J. Chem. Phys.* **61**, 2695-2699 (1974).

[17] P. Segur, F. Massines, The role of numerical modelling to understand the behaviour and to predict the existence of an atmospheric pressure glow discharge controlled by a dielectric barrier, *Proc. 13th Int. Conf. on Gas Discharges and their Applications (Glasgow, UK)*, 15-24 (2000).

[18] C. Khamphan, P. Segur, F. Massines, M.C. Bordage, N. Gherardi and Y. Cesses, Secondary electron emission by nitrogen metastables states in atmospheric-pressure glow discharge, *Proc. 16th Int. Symp. on Plasma Chemistry (Taormina/Italy)*, CD-ROM (2003).